Extraction and characterization of vascular bundle and fiber strand from date palm rachis as potential bio-reinforcement in composite

Haithem Boumediri, Abderrezak Bezazi, Gilberto Garcia del Pino, Abdelkrim Haddad, Fabrizio Scarpa, Alain Dufresne

Extraction and characterization of vascular bundle and fiber strand from date palm rachis as potential bio-reinforcement in composite

Haithem Boumediri,[a] Abderrezak Bezazi,[a] Gilberto Garcia Del Pino,[b] Abdelkrim Haddad,[a] Fabrizio Scarpa,[c] Alain Dufresne[d*]

[a] Laboratoire de Mécanique Appliquée des Nouveaux Matériaux (LMANM), Université 8 Mai 1945, Guelma, Algeria

[b] Department of Mechanical Engineering, State University of Amazonas, Manaus-AM/Brazil, Brazil

[c] Department of Aerospace Engineering, University of Bristol, Queens Building, University Walk BS8 1TR Bristol, UK.

[d] Univ. Grenoble Alpes, CNRS, Grenoble INP, LGP2, F-38000, France.

* Corresponding author: alain.dufresne@pagora.grenoble-inp.fr

Keywords: Date palm fibers; Vascular bundles; Fiber strands; Physicochemical analysis; Surface roughness; Tensile properties**.**

Abstract

Date palm rachis fibers are rich in cellulose, relatively inexpensive, and readily available in Algeria. The aim of this study is to investigate the morphology, structure, mechanical and physicochemical characteristics of both vascular bundles and fiber strands extracted from date palm rachis. The difficulties encountered are associated to the extraction of the fibers without damaging them. The study focuses on the morphological and surface roughness analysis using optical and scanning electron microscopies (SEM), and a non-contact 3D profiler. The chemical, physical and thermal properties have been studied using Fourier-transform infrared (FTIR) spectroscopy, energy dispersive X-ray spectroscopy (EDX), X-ray diffraction (XRD), thermogravimetric analysis (TGA), and differential scanning calorimetry (DSC). The mechanical properties were accessed by tensile tests and they were analyzed using two-parameter Weibull distribution.

INTRODUCTION

The date palm (Phoenix dactylifera L.) is a monocotyledonous flowering plant of the family Palmates (Arecaceae), one of the most important cultivated crops in North Africa and the Middle East (NAME) (Chao & Krueger, 2007). According to Graziano da Silva, General Director of the Food and Agriculture Organization (FAO), the date palm is a symbol of life in NAME. Palm trees play an important role in the economy of the region, with the top ten producing countries accounting for approximately 90% of the global date production (Chandrasekaran & Bahkali, 2013; Ghnimi, Umer, Karim, & Kamal-Eldin, 2017).

Algeria, which is the largest country in Africa and in the Arab world, is among the leading countries in the cultivation and production of palms dates. It is the world's fourth-largest date producer with a total of more than 20 million palm trees and was responsible for more than 14% of the global date production in 2017, with an increase of more than 83% from 2012 to 2017, as confirmed by the Algiers Chamber of Commerce and Industry (Boumediri et al., 2017).

However, as reported in 2011 by (Agoudjil, Benchabane, Boudenne, Ibos, & Fois, 2011) this crop generates a large amount of by-products, such as: (a) the leaves: petiole, rachis, leaflets; (b) the trunk; (c) the products obtained from the bunches (fruit bunch branch of palm, date seeds). It can subsequently produce approximately 40 kg of residue per individual date palm tree annually (Mallaki & Fatehi, 2014). This huge residue amount is not exploited because it is often disposed of by burning or is considered as animal feed or waste and it has been rarely used in handicrafts such as basketry, crates, ropes and traditional construction (Al-Oqla & Sapuan, 2014; Bouguedoura, Bennaceur, Babahani, & Benziouche, 2015).

For researchers interested in lignocellulosic fibers, this agricultural residue is a natural wealth, that can be exploited and valued in different ways such as the reinforcement for biocomposite materials for many application and various industries sectors (Al-oqla,

Alothman, Jawaid, Sapuan, & Es-Saheb, 2014; Anwar, Gulfraz, & Irshad, 2014; Jawaid & Abdul Khalil, 2011; Rabetafika, Bchir, Blecker, & Richel, 2014). This is due to their unique collective advantages, which include easy availability, recyclability, environmental friendliness, biodegradability, low cost, low density, good thermal stability, and reasonable strength and stiffness (Jayaramudu, Guduri, & Varada Rajulu, 2010; Manimaran, Saravanakumar, Mithun, & Senthamaraikannan, 2016).

In fact, recent years have been marked by a sharp increase in studies and work on the use of farming-based waste from the date palm. Studies have focused on the outer layer of the date palm stem called mesh, due to their availability in the form of fiber with the objective of using these fibers as reinforcement for composites materials (Al-Kaabi, Al-Khanbashi, & Hammami, 2005; Al-Khanbashi, Al-Kaabi, & Hammami, 2005; Alawar, Hamed, & Al-Kaabi, 2009; Alsaeed, Yousif, & Ku, 2013; Oushabi et al., 2017). Amroune et al. investigated the mechanical properties of the fiber of date palm fruit branches for use as potential reinforcement for polymer composites (Amroune et al., 2015). Other investigations are dedicated to the use of date palm wood, petioles and leaves by cutting or hammering into small pieces as material for the manufacture of particleboard (Almi, Lakel, Benchabane, & Kriker, 2015; Saadaoui, Rouilly, Fares, & Rigal, 2013). Also, Khiari et al. study the application date palm rachis as a source of lignocellulosic biomass for the production of pulp and paper (Khiari, Mhenni, Belgacem, & Mauret, 2010). Unfortunately, there is scarce information available about the utilization and properties of the date palm rachis fibers as a potential eco-friendly bio-reinforcement for bio-composites materials.

According to Agoudjil et al. an amount estimated to more than 800,000 tons of residues is produced per year in Algeria. Botanic experts reported that each date palm tree can produce an average of thirteen new rachis and petioles per year (Agoudjil et al., 2011; Nasser et al., 2016) that corresponds to an average mass of 9.75 kg and 4.4 kg, respectively (Darwish,

Mansour, & Elmously, 2018). Based on this information, the cultivation of date palm can then produce around 200,000 tons of fronds and 90,000 tons of petioles, which are available per year in Algeria. There are more than 950 varieties of date palms in Algeria and the analysis of their production by category shows that the variety of Ghars palm tree represents up to 10% of the total production in Algeria (Bouguedoura et al., 2015).

This variety of date palm, with very good commercial value and availability, has not been sufficiently explored. This is why it has been chosen to be the aim of this investigation. The analysis of the rachis cross section morphology leads to identify for the first time the existence of two main types of date palms rachis fibers namely: vascular bundles (VBs) and fiber strands (FSs) and showing their location in the rachis. The first part of this work is devoted to the development a new method of extracting VBs and FSs fibers from the Ghars rachis without any damaging or breaking of them. To the author's knowledge, this is the first investigation permitting to provide a comparison and detailed analysis of the two types of Ghars rachis fibers (VBs and FSs), with emphasis on their physicochemical, thermal and tensile mechanical properties. Furthermore, their morphology and roughness have been identified and compared. To do this, various techniques has been used to characterize the extracted fibers by scanning electron microscopy (SEM), non-contact 3-D profiler, thermogravimetric analysis (TGA), differential scanning calorimetry (DSC), Fourier-transform infrared (FTIR) spectroscopy, energy dispersive X-ray (EDX) spectroscopy, X-ray diffraction (XRD) and tensile test. To the author's knowledge, the ultimate tensile stress of FSs obtained show the greatest values compared to VBs and also to all the fibers date palm existing in the literature.

MATERIALS AND METHODS

Materials

There are more than 950 varieties of date palm in Algeria such as Deglet Nour, Ghars, Fergus

and Mech Degla (Bouguedoura et al., 2015) and they can be classified into 04 categories from the commercial point of view and their availability:

- *Variety of very good commercial value*, such as: Deglet-Nour, Ghars, Degla-Beida, Tafenoquine, Itima, Mech-Degla, etc ...
- *Ordinary variety*, such as: Arechti, Boudheroua, Taouri, Hamraia and Ksebba, etc…
- *A rare variety, less value*, *very little available*: Oum-rouah, Oum-Soualef, Oum-aidjet, Oum-Chouika, Azenchi, etc ...
- *A rare variety, not available* (limited number to recently discovered), such as introduced foreign varieties: Zohdi, Halami, Ftemi, Alig, etc ...

Apart from being classified by commercial and availability, another classification for date palm is based on the external quality of the fruit of the crops in three classes (Biglari, AlKarkhi, & Easa, 2008):

- Palm trees producing *soft dates*: which are aqueous, of fibrous texture such as: Ghars, Hamraia, Itima, Zegraia, etc ...
- Palm trees producing *semi-dry date*s or *semi-soft dates*: which dry up such as: Deglet-Nour, Arechti, Sebaa, Boudraa, Amdj-Zenina, Deglet-Messaoud, etc ...
- Palm trees producing *dry dates* or *hard dates*: which harden on the tree and have a floury texture, such as: Degla-Beida, Laalami, Lahlou, Deglet-Zohra, Arelou, etc…

In this work, we used leaves of a female palm tree Ghars, this variant of date palm tree represents up to 10% of the total production in Algeria. It is known by its earliness in ripening, its productivity and the ability of this tree to withstand large amounts of alkali and much neglect. This variety of date palm has a very good commercial value and great availability but has not been sufficiently explored. The Ghars rachis used was collected in November 2017 from a local farm in El-Oued located in the south of Algeria, this farm used brackish water for irrigation. The rachis taken from the palm tree (Figure 1a) was obtained by

removing the leaflets and it was cut about 20 cm in length using a knife. The fibers were extracted from the rachis by a manual peeling process. After 150 min of boiling in an autoclave at 120 °C the fibers were extracted from the rachis outer and inner peripheries, and it was observed that it consisted of two types of fibers: vascular bundles (VBs) and fiber strands (FSs) VBs and FSs looks like for the anatomy of pineapple leaves (Mohamed, Sapuan, Shahjahan, & Khalina, 2010). Then, the separated fibers were washed thoroughly using water and then sun dried for one week to ensure maximum moisture removal. Finally, the dried VBs and FSs fibers were collected as shown in Figure 1d for further investigations.

Figure 1. Photographs of (a) date palm tree, (b) date palm rachis and leaflets, (c) cut rachis, and (d) vascular bundles (VBs) and fiber strands (FSs).

Characterization

Morphology and surface elemental composition (SEM–EDX analysis). The micrographs were obtained with an environmental scanning electron microscope (SEM) (FEI Quanta 250) equipped with a secondary electron large-field detector (LFD). Micrographs were obtained under low vacuum mode (at a pressure of 40 Pa) under an accelerating voltage between 10 to 20 kV, with a spot size of 3-5 nm and a working distance ranging from 9 to 12 mm. Elemental analysis of the fiber surface was performed by energy dispersive X-Ray spectroscopy analysis (TEAM-EDX Model) to access the amount of existing elements and results were expressed in weight and atomic percent.

Topographic characterization. The surface roughness of VBs and FSs fibers was optically scanned in 3D using a confocal white light sensor with a high-resolution profilometer (CT-100, Cyber Technologies). The samples were scanned with a step size of 5 μm for an illumination time of 0.5 ms. After scanning, the measured roughness characteristics were analyzed with the SCAN-SUITE software.

Fourier-transform infrared (FTIR) spectrometry. FTIR spectra were obtained with FTIR spectrometer (Nicolet iS10 from Thermo Fisher Scientific equipped with a Golden Gate single reflection ATR accessory) in the wavenumber range 4000-500 cm^{-1} at a temperature of 25°C and 55% relative humidity. All spectra were collected with a 1 cm^{-1} wavenumber resolution after 32 continuous scans. Spectrum analysis was performed with Smart OMNI-Transmission accessory (Software OMNIC 9.5).

Thermogravimetric analysis (TGA). Thermogravimetric analysis (TGA) and derivative thermogravimetry (DTG) of the fiber samples were carried out using a TGA/DSC 3+ (METTLER TOLEDO). Approximately 10 mg of the sample were filled in ceramic alumina crucible capsule and heated from 30°C to 600°C at a constant heating rate of 10 °C/min, under nitrogen atmosphere at a flow rate of 20 mL/min to prevent any oxidative degradation. The DTG data were also obtained from the analysis using STARe-Evaluation Software.

Differential scanning calorimetry (DSC). Differential scanning calorimetry (DSC) analysis was performed using DSC 3+ (METTLER TOLEDO). The equipment was calibrated with aluminum oxide before analysis. The sample (weighing approx. 6 mg) was encapsulated in a hermetic aluminum pan before analysis, and an empty pan was used as reference. The sample was then heated from 30°C to 600°C at a heating rate of 10 °C/min. The nitrogen source was adjusted to a flow of 100 mL/min. All thermograms were analyzed using STARe-Evaluation Software.

X-ray diffraction (XRD) analysis. Powder X-ray diffraction (XRD) patterns of the samples were obtained using an X-ray PANalytical Empyrean diffractometer equipped with a PIXcel-3D detector and Cu-Kα radiation (λ = 1.540598A°). The generator was operated at 45 kV voltage and 40 mA current. Powder samples were mounted on a sample holder and scanned from 10° to 40° (2θ angle range) at a scan rate of 5°/min. The length of the specimen used was 10 mm and the measurement temperature was about 23°C.

The crystallinity index (C.I.) and percentage of crystallinity (%Cr) were calculated based on the Segal method (Segal, Creely, Martin, & Conrad, 1959) using the following equations (1) and (2), respectively:

$$C.I. = (I_{002}-I_{am})/I_{002} \times 100 \qquad \text{(Eq.1)}$$

$$Cr\ (\%) = (I_{002}/I_{002}+I_{am}) \times 100 \qquad \text{(Eq.2)}$$

where I_{002} is the maximum intensity diffraction of the 002-lattice reflection of the crystallographic form of cellulose at $2\theta=22°$, and I_{am} the minimum intensity of the amorphous material at an angle of approximately 18.5° in the valley between the peaks.

The crystallite size (CS) for VBs and FSs was calculated using Scherrer's equation (Maache, Bezazi, Amroune, Scarpa, & Dufresne, 2017):

$$CS = k \lambda / \beta_{002} \cos \theta \qquad \text{(Eq.3)}$$

where CS is the crystallite size (nm), k is the Scherrer constant (0.9), λ is the wavelength of X-ray beam (1.5405 A°), β is the full width half maxima (FWHM) of peak diffraction (in rad) and θ is the diffraction angle. XRD data were deconvoluted using MagicPlot-Pro 2.7.2 software by adjusting one amorphous and three crystalline peak sum for each original curve via Gaussian deconvolution.

Fiber density. The density (ρ_f) for VBs and FSs fibers was calculated by liquid immersion test using pycnometer with distilled water (ASTM D2320-98) and was determined by the following equation (4):

$$\rho_f = [(m_2-m_1)/(m_3-m_1)-(m_4-m_2)]\rho_{wt} \qquad \text{(Eq.4)}$$

where m_1, m_2, m_3, m_4 and ρ_{wt} are the mass of empty pycnometer (g), the mass of pycnometer with fibers (g), the mass of pycnometer with distilled water (g), the mass of pycnometer with fibers and distilled water (g), and the density of distilled water (0.997 g/cm^3), respectively.

Technical fiber tensile tests. The tensile tests were conducted using Zwick/Roell universal testing machine Z2.5 equipped with a 200 N load cell attached to an automatic data acquisition system. 20 samples were analyzed for each group according to ASTM D3822-07 for a fiber length of 30 mm at a constant speed of 1 mm/min. All tests were carried out at a temperature of 23 °C and a relative humidity of approximately 45%. The cross-sectional area was evaluated from the diameter measured using an optical microscope (Motic-BA310 Met, Motic Images Plus 2.0 software) at three different points along the effective fiber length. The statistical analysis of tensile strength values has been analyzed by two parameters Weibull distribution model. The obtained results were treated by Minitab software.

RESULTS AND DISCUSSION

Morphological analysis

Figures 2a and 2b show SEM micrographs of the cross-section at the base and 20 cm before the tip of the date palm rachis, respectively. The micrographs clearly show a gathering of several fibers dispersed and separated by chlorenchyma cells. However, there is a clear difference in the microstructure of these fibers, which can be classified into two types, the first called vascular bundle (VBs) which is the thicker one and that appears in the middle of the main voids, while the second called fiber strand (FSs) is the thinnest that do not contain any main voids. It is worth noting that the parenchyma cells of the base rachis are much denser compared to the tip from the rachis of date palm.

Figures 2c and 2d display the cross-section of VBs and FSs from the rachis of date palm, respectively. The microstructural observation carried out for VBs showed that the surface area is elliptical nearly circular in shape, the VBs being composed of two main voids with diameter ranging from 100 to 150 µm with a large number of spherical microfibrils with a smaller diameter in the range 6-22 µm, aligned and bonded together by lignin, pectin and other non-cellulosic materials (Manimaran, Senthamaraikannan, Sanjay, Marichelvam, &

Jawaid, 2018). FSs are composed of several individual microfibrils with a diameter in the range 4 to 12 µm, compactly arranged to form a technical fiber whose shape is approximately cylindrical and whose diameter was found in the range 80 to 120 microns.

The SEM micrographs of the surface (longitudinal direction) for VBs and FSs are depicted in Figures 2e and 2f, respectively. The presence of some impurities randomly distributed is observed on the surface of VBs and FSs fibers, their existence resulting from the extraction technique. The fiber structure exhibits an alignment in the direction of the fiber axis, in the shape of a regularly distributed semi-rectangular and square tray, along with the length of the lines on the surface of the fibers. Further, it shows small void holes or pits not uniformly spaced and it has the shape of an almost circular elliptical at the surface. In general, this type of structure is similar to other vascular fiber bundles such as arundo fibers (Fiore, Scalici, & Valenza, 2014) and to fiber strands like banana fibers (Kambli, Basak, Samanta, & Deshmukh, 2016).

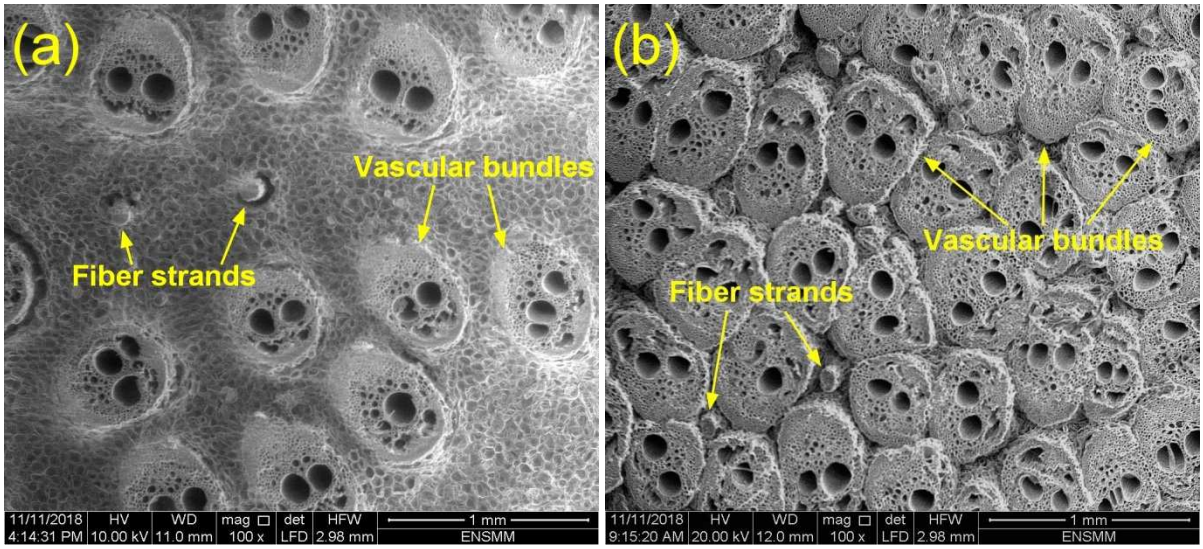

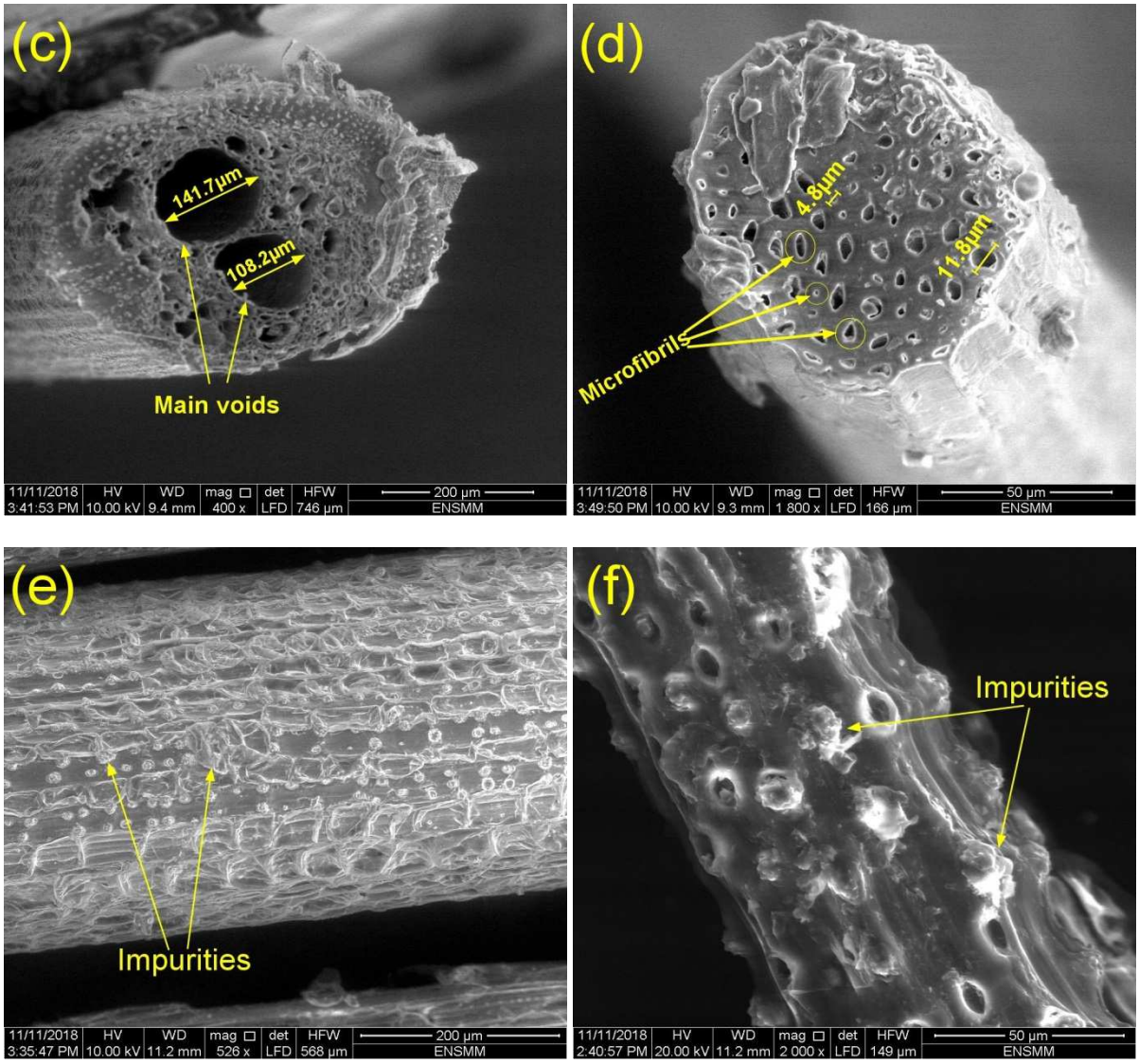

Figure 2. SEM micrographs of the cross-section at: (a) the base of the rachis, and (b) 20 cm before the tip of the rachis. SEM micrographs of the cross-section for (c) VBs (d) FSs and longitudinal view for (e) VBs, and (f) FSs.

EDX analysis

Figures 3a and 3b show the spectral imaging generated by energy dispersive X-ray spectroscopy (EDX) for VBs and FSs, respectively. The fibers consist of elements such as carbon (C), oxygen (O), small amounts of sodium (Na), aluminum (Al), silicon (Si) and traces of chlorine (Cl), potassium (K), calcium (Ca) and the existence of sulfur (S) only in FSs fibers.

253

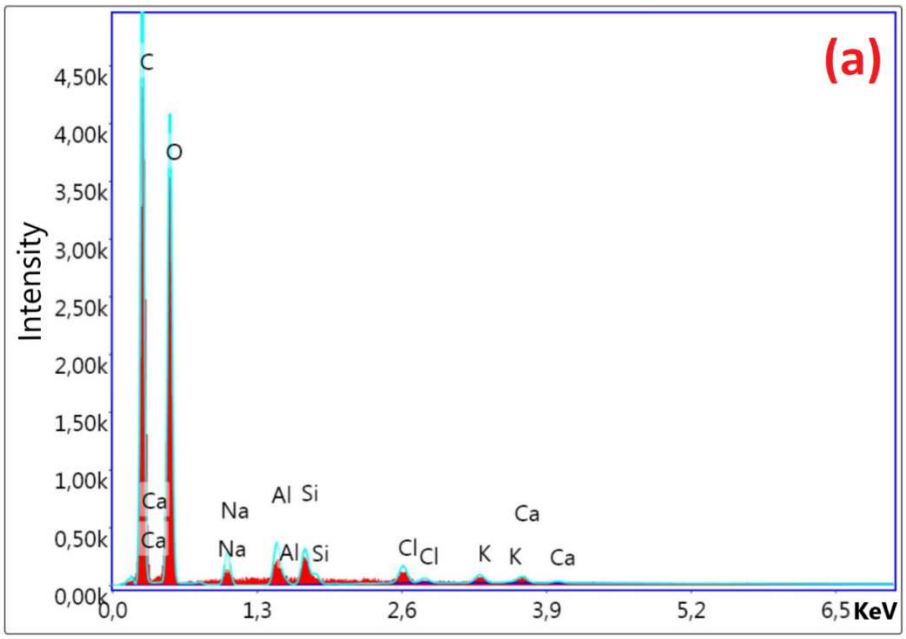

254

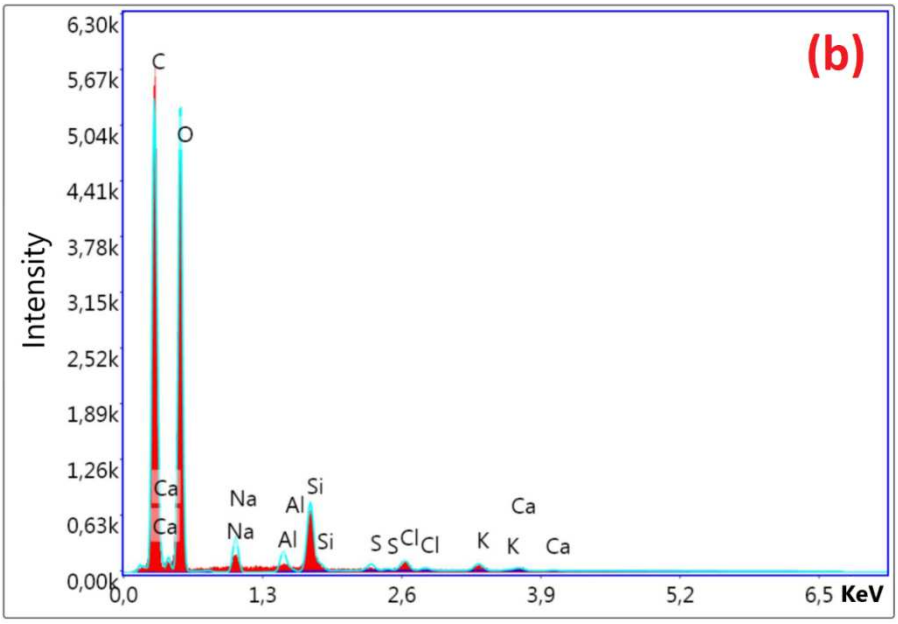

255 **Figure 3.** EDX analysis for (a) VBs and (b) FSs.

256 Table 1 reports the results for the weight content and atomic content calculated from the peak
257 areas for all elements. It indicates a similar composition for both fibers. Carbon and oxygen
258 are the main constituents because they are the main components for natural fiber structures
259 (Kambli et al., 2016), that corresponds to the known chemical composition of lignocellulosic
260 fibers.

261 **Table 1.** Weight (W%) and atomic percentage (A%) for VBs and FSs fibers compared to

other lignocellulosic fibers.

Fiber		Element										Reference
		C	O	Na	Al	Si	Cl	S	Mg	K	Ca	
Vascular bundles	W%	50.14	46.41	1.85	0.86	0.47	0.14			0.06	0.05	Present work
	A%	57.88	40.22	1.12	0.44	0.23	0.06			0.02	0.02	
Fiber strands	W%	50.1	46.21	2.03	0.41	0.97	0.11	0.07		0.07	0.04	
	A%	57.89	40.09	1.22	0.21	0.48	0.04	0.03		0.03	0.01	
Furcraea foetida	W%	66.34	72.50									(Manimaran et al., 2018)
	A%	33.57	27.50									
Cornhusk fiber	W%	62.54	36.80			0.20			0.13		0.33	(Kambli et al., 2016)
	A%	69.17	30.56			0.10			0.07		0.11	
Cotton fiber	W%	46.1	53.2									
	A%	53.9	46.8									
Jute fiber	W%	55.68	43.89			0.11		0.18				
	A%	62.72	37.11			0.06		0.08				

Surface roughness analysis

Figures 4a and 4b show the 3D roughness surface texture, 2D line diagram for roughness measurement and profilometry results conducted according to ISO 4287 for VBs and FSs fibers, respectively. The visual inspection of 3D topographic images makes it easy to observe the variation in peak value on the surface represented by red color because of the impurities, inorganic substances and the existence of lignin (Manimaran et al., 2018). The area of valleys found in the 3D roughness surface texture (blue color) is due to the presence of voids in VBs and holes or pits in FSs.

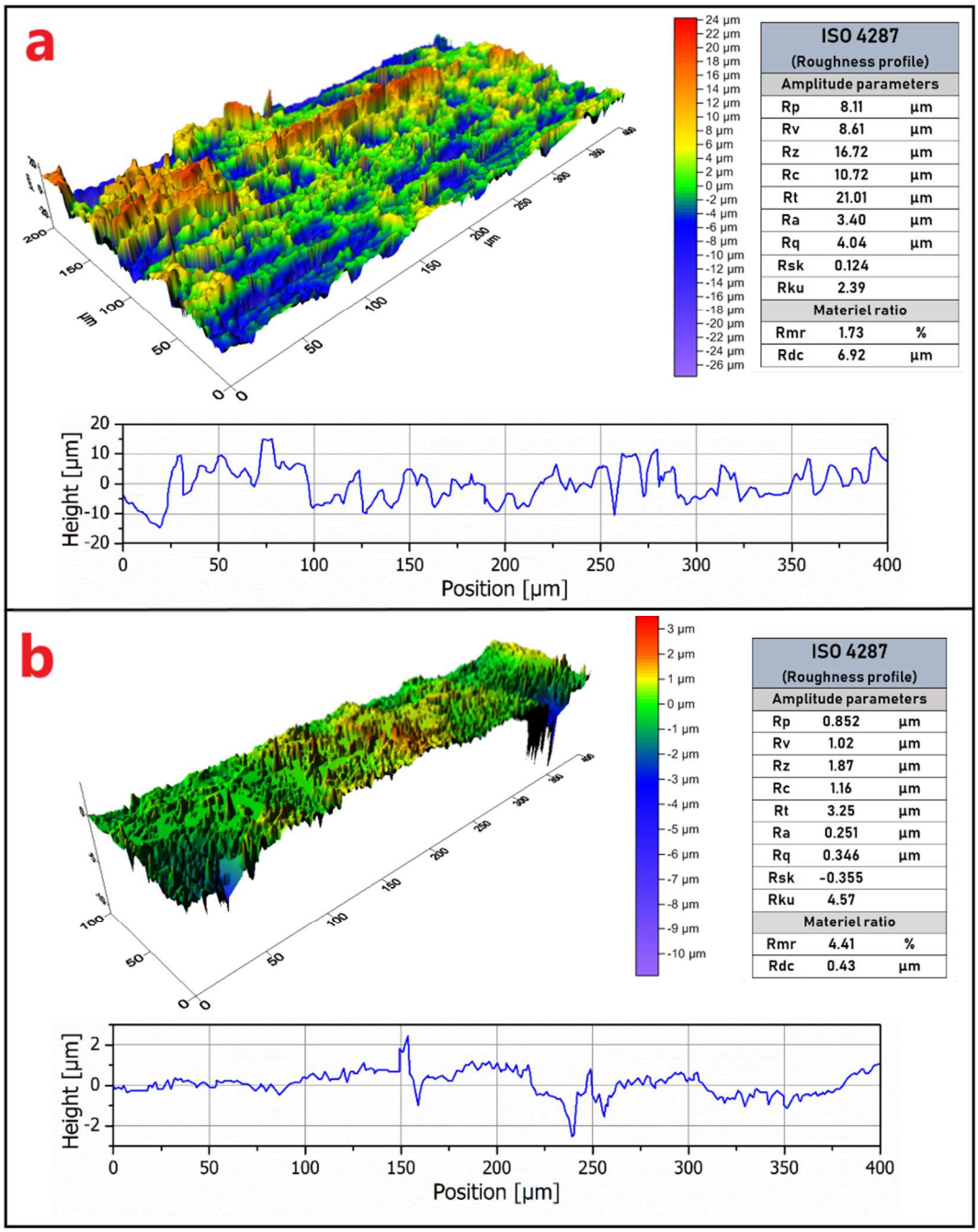

Figure 4. 3D surface roughness and 2D line diagram for roughness for (a) VBs and (b) FSs. The 2D line diagram for VBs and FSs show a non-uniform surface roughness along the fiber length. The profilometry results were evaluated and found to be as follow: for VBs (Ra = 3.40 µm, Rz = 16.72 µm, Rq = 4.04 µm, Rt = 21.01 µm) and it was lowest for FSs (Ra = 0.251 µm, Rz = 1.87 µm, Rq = 0.346 µm, Rt = 3.25 µm). The surface roughness for VBs was higher than for other natural fibers like Ra = 0.613 µm for Coccinia grandis stem fiber (Jebadurai, Raj, Sreenivasan, & Binoj, 2018), Ra = 0.611µm for Veldt-grape stem fiber

(Mayandi et al., 2015) and Ra = 0.625 μm for Cyperus pangorei fibers (Mayandi, Rajini, Pitchipoo, Jappes, & Rajulu, 2016), but for FSs it was slightly lower. It was reported that the surface roughness is one of the important properties for enhancing mechanical interlocking between fiber and matrix when used as reinforcement in composite materials (Maache et al., 2017).

FTIR analysis

The FTIR spectra recorded for VBs and FSs of date palm rachis are represented in Figure 5a. Both fibers presented the typical vibration bands of different chemical functional groups of lignin, hemicellulose and cellulose. The strong and broad peak at 3346 cm^{-1} is associated with the O-H stretching vibration and hydrogen bond of the hydroxyl groups (Amroune et al., 2015). The double peak observed at 2925 and 2854 cm^{-1} are assigned to CH_2 asymmetrical and symmetrical stretching, respectively. The absorption band centered at 1734 cm^{-1} can be attributed to the C=O group and stretching vibration of ester group in hemicellulose (Bezazi, Belaadi, Bourchak, Scarpa, & Boba, 2014). The small band at 1646 cm^{-1} corresponds to the O-H bending of absorbed water. Following three peaks are characteristic of lignin: 1604 cm^{-1} (aromatic skeletal vibration of lignin plus C=O stretching), 1508 cm^{-1} (C=C stretching of aromatic skeletal vibration of Lignin), 1456 cm^{-1} (C-H deformation (asymmetric) and aromatic vibration in lignin) (Amroune et al., 2015; Saravanakumar, Kumaravel, Nagarajan, & Moorthy, 2014). The absorbance at 1423 cm^{-1} is attributed to the presence of C–H deformation in lignin and CH_2 symmetric bending in cellulose (Maache et al., 2017). The absorption band at 1373 cm^{-1} is assigned to the bending vibration of the C-H group of the aromatic ring in hemicellulose and cellulose (Bezazi et al., 2014). The absorbance at 1319 cm^{-1} is attributed to the CH_2 rocking vibration in cellulose (Saravanakumar et al., 2014). The tiny peak at 1241 cm^{-1} is assigned to the C-O stretching of acetyl group in lignin (Bezazi et al., 2014). The two peaks observed at 1160 cm^{-1} and 1033 cm^{-1} are attributed to the C-O-C

asymmetric stretching vibration and C–O stretching ring in cellulose and hemicellulose, respectively (Saravanakumar et al., 2014). A small peak at 897 cm^{-1} is attributed to the β-glycosidic linkages between the monosaccharides. The small absorption peak at 605 cm^{-1} is associated with C-OH out of plane bending in cellulose (Fiore et al., 2014).

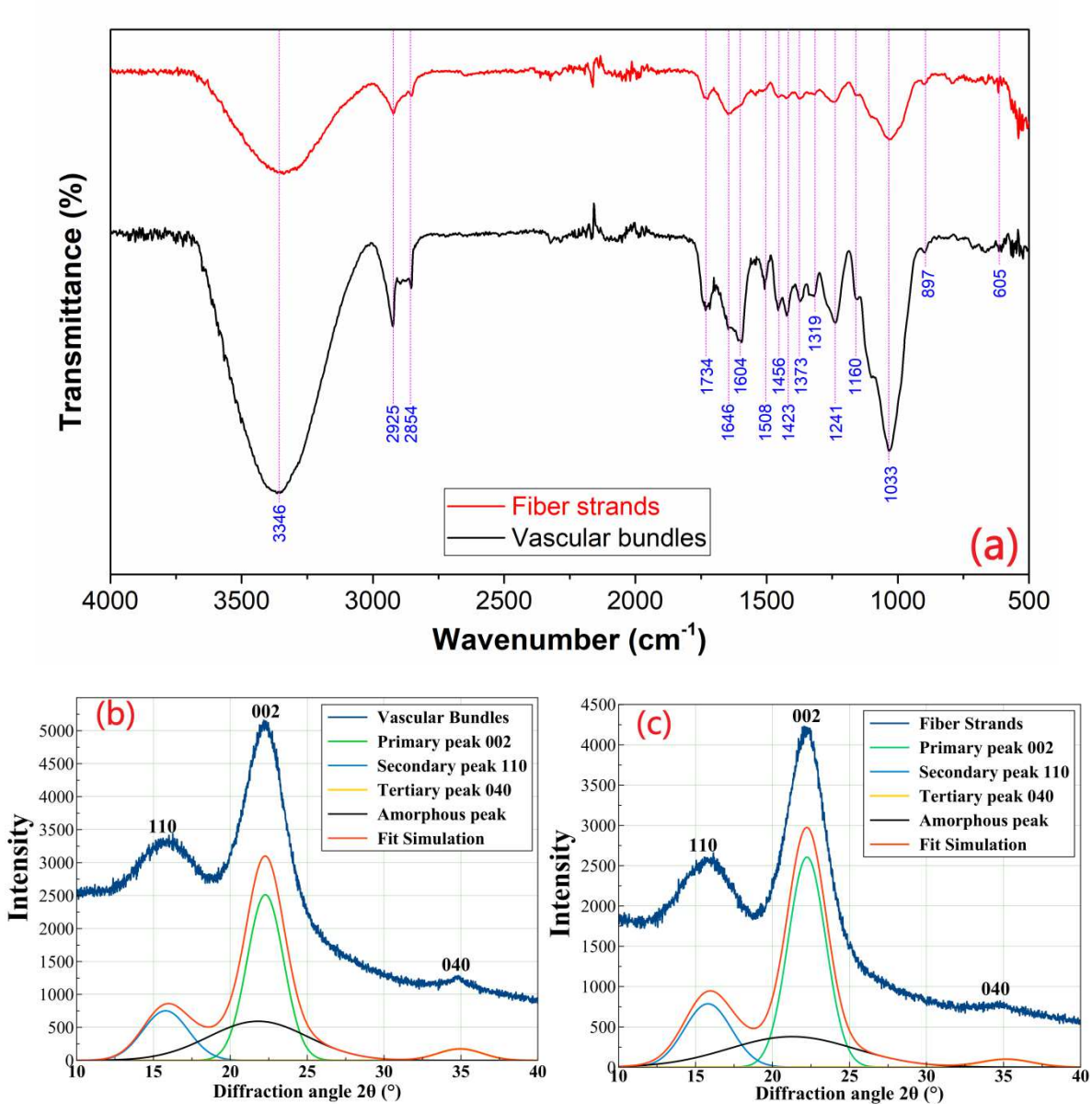

Figure 5. (a) FTIR spectra for VBs and FSs, and XRD patterns for (b) VBs and (c) FSs.

XRD analysis

The diffraction patterns obtained for VBs and FSs between 10 and 40° are shown in Figures 5b and 5c, respectively. The deconvolution of the X-ray diffraction profiles showed the

315 presence of three peaks and an amorphous bump. For both VBs and FSs the highest intensity
316 peak was observed at 2θ = 22.2°, average intensity peak at 2θ = 15.86° and a peak of low
317 intensity at 2θ = 35°, which were assigned to the (002), $(10\bar{1})$, and (040) crystallographic
318 planes (Jebadurai et al., 2018).
319 The crystallinity index (C.I.) was found to be 47.82% and 56.68% for VBs and FSs samples,
320 respectively, which means that FSs exhibit a better order of cellulose crystals at the fiber axis
321 compared to VBs. On the other hand, the percentage of crystallinity (%Cr) for VBs and FSs
322 was found equal to 65.71% and 69.77%, respectively. In addition, the crystallite size (CS)
323 for VBs and FSs was calculated using Scherrer's equation and the value was found to be 5.78
324 nm and 5.63 nm, respectively, which is smaller than the value reported for Furcraea foetida
325 (28.36 nm), Prosopis juliflora bark (15 nm), but higher than for *Juncus effusus L.* (3.6 nm)
326 and Coccinia grandis stem (1.91 nm) as reported by (Jebadurai et al., 2018; Maache et al.,
327 2017; Manimaran et al., 2018; Saravanakumar, Kumaravel, Nagarajan, Sudhakar, &
328 Baskaran, 2013). The obtained results are summarized in Table 2 and compared to (Roy et
329 al., 2012; Wei & Meyer, 2015)
330 **Table 2.** Calculated and experimental crystalline parameters from XRD diffractograms of
331 fibers.

Type of fiber	Peak position (°)	FWHM (rad)	Area (%)	Crystallinity (%)	Crystalline index (%)	Crystallite size (nm)	Reference
Vascular bundles	15.79	1.74	2789.23				Present work
	22.28	1.40	7487.62	65.71	47.82	5.78	
Fiber strands	15.81	1.79	3006.61				
	22.24	1.44	7980.62	69.77	56.68	5.63	
Sisal fiber	16,81	4.89					(Wei & Meyer, 2015)
	22,31	3.37		77.6	71.2	3.37	
Jute fiber	15.62	4,23	42.05				(Roy et al., 2012)
	23.36	2.89	57.94	53.7		2.78	

332

TGA analysis

Thermogravimetric analysis (TGA) and derivative thermogravimetry (DTG) are thermal analysis techniques used to measure the weight loss of a material when heated, i.e. to access its thermal stability, and characterize its decomposition temperature.

Figure 6 presents the TG and DTG curves for VBs and FSs, which show four weight loss stages. The first stage associated with a small weight loss (8.10%) for VBs and (7.00%) for FSs, corresponds to the dehydration phase that was observed in the temperature range 30-120 °C. This stage was attributed to the evaporation of adsorbed moisture, which is related to the hydrophilic nature of lignocellulosic materials (Fiore et al., 2014). Then, it can be concluded that both VBs and FSs can be considered thermally stable up to 230 °C and 220, respectively. The thermal stability of lignocellulosic fibers is important for the processing and usage of these materials as a reinforcement in biocomposites (Maache et al., 2015). In the second stage, the degradation of hemicelluloses was recorded in the temperature range 220-325 °C with a weight loss of 29% for VBs and in the temperature range 220-300 °C with a weight loss of 22% for FSs (Martin, Martins, Da Silva, & Mattoso, 2010; Saravanakumar et al., 2013). It is confirmed by the observation of a peak in the DTG curves at 296 °C for VBs and 280 °C for FSs. Afterward, the major weight loss occurred rapidly in the third degradation stage, corresponding to the decomposition of cellulose in the temperature range 325-490 °C associated with a weight loss of 39.00% for VBs and in the temperature range 300-480 °C with a higher weight loss of 41.51% for FSs. The DTG plots showed distinct peaks at 360 °C for VBs and 345 °C for FSs (Jebadurai et al., 2018). Lastly, the final stage corresponding to the decomposition of lignin was observed in the temperature range 400-485 °C with a small weight loss for VBs (10%) and in the temperature range 380-465 °C with a smaller weight loss for FSs (7%) (Roy et al., 2012). In addition, amounts of charred residues were observed for VBs (16.66%) and FSs (18.28%).

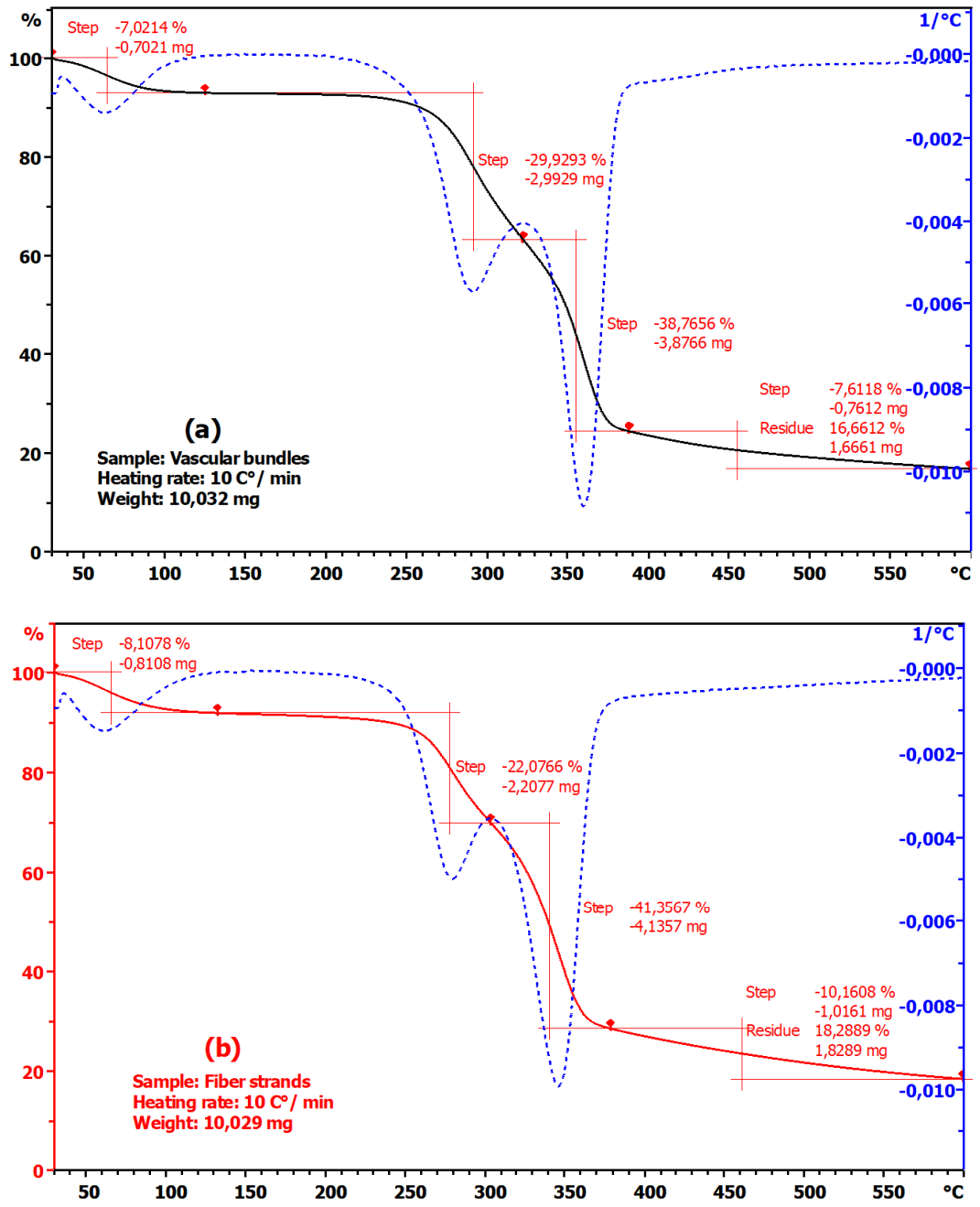

Figure 6. TGA/DTG curves for (a) VBs and (b) FSs.

DSC analysis

Differential scanning calorimetry (DSC) analysis was carried out for both VBs and FSs for determining its thermal behavior. DSC analysis allows observing physical changes through the absorption and release of thermal energy during heating, which allows the identification of thermal transitions. Figure 7 shows the DSC curves obtained for VBs and FSs presenting the endothermic and exothermic processes where some differences can be noted. The first

endothermic peak was centered at 92°C and 88°C for VBs and FSs, respectively. It corresponds to the loss/evaporation of absorbed water (Belaadi, Bezazi, Bourchak, Scarpa, & Zhu, 2014). The corresponding enthalpy calculated by integrating the peak was 217 J/g and 209 J/g for VBs and FSs, respectively.

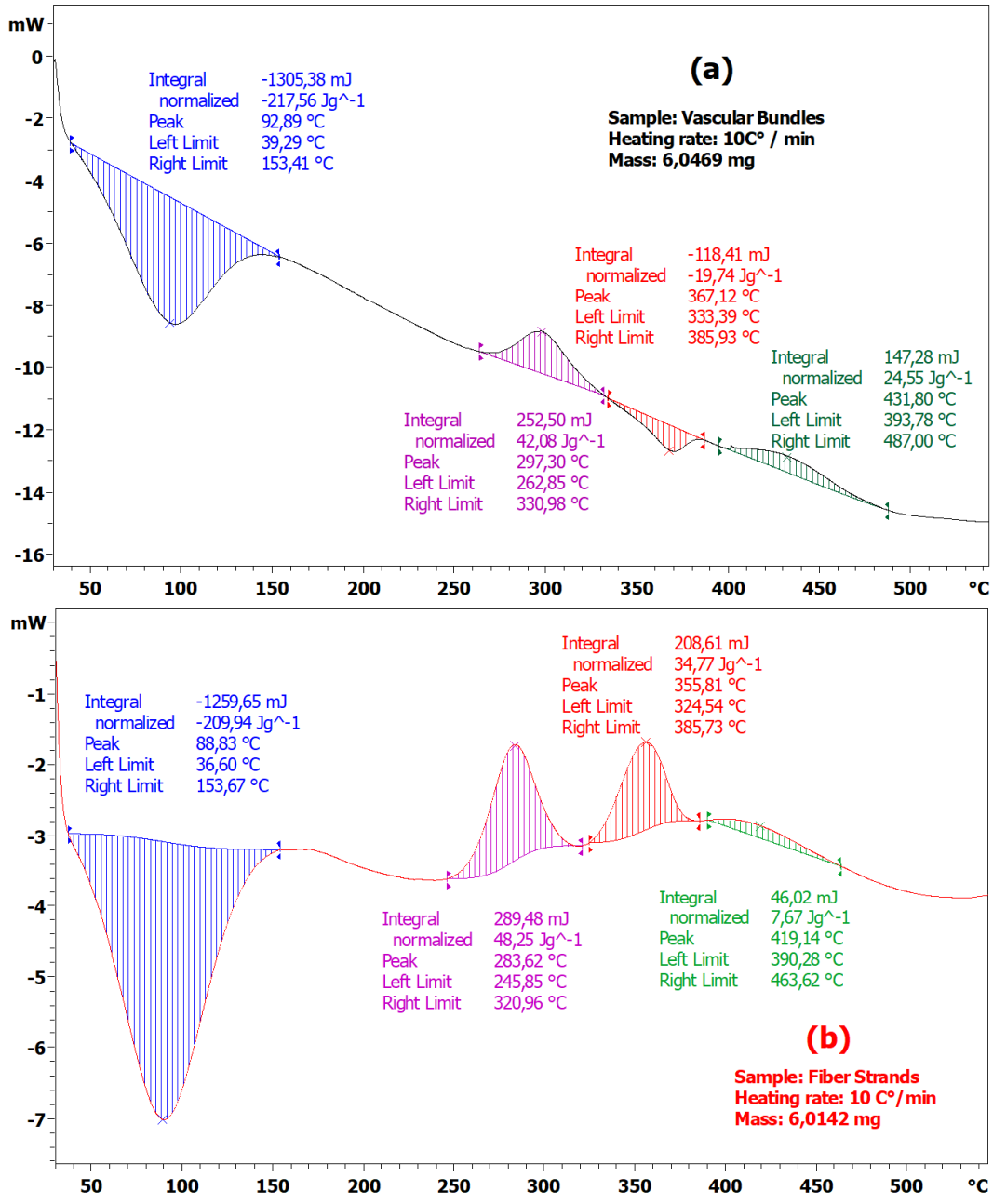

Figure 7. DSC curves for (a) VBs and (b) FSs.

The exothermic peak observed at 297°C and 283°C for VBs and FSs, respectively, is mainly due to the degradation of hemicelluloses present in the samples which is associated with an

enthalpy of 42 J/g for VBs and 48 J/g for FSs (Martin et al., 2010). Then a different behavior is observed between VBs and FSs with an endothermic peak around 367°C for the former and exothermic peak around 355°C for the later. According to DTG results this signal should correspond to the degradation of cellulose and the associated enthalpy is 19 J/g for VBs while it is 34 J/g for FSs (Roy et al., 2012). Finally, a small exothermic peak observed at 431 ºC for VBs and 419 ºC for FSs is mainly due to the thermal decomposition of lignin, were a much higher enthalpy (24 J/g) is reported for VBs than for FSs (7 J/g).

Technical fiber tensile tests and statistical analysis

The typical stress-strain curves for VBs and FSs under tensile tests behave quasi-linearly and non-linearly, respectively, until failure (Figure 8a). It is worth noting that the mechanical properties of FSs are largely better compared to VBs. Due to the dispersion in the obtained results, it was deemed necessary to analyze them statistically using two-parameters Weibull distribution fit plots of the test data for all the 20 trials with 95% confidence level curves for tensile strength, Young's modulus and strain at failure. The results are presented in Figure 8b, 8c, and 8d, respectively, for VBs and FSs having an average diameter of 520±72µm and 88±12µm, respectively, with low density of 0.914 g/cm^3 and 0.922 g/cm^3, respectively. The Weibull distribution provides a reasonable approximation of the experimental data for evaluating the mechanical properties of different natural fibers. The experimental results obtained for VBs and FSs were found to be 129.1±47.3 MPa and 530.5±115.2 MPa for the ultimate tensile strength, 5.88±1.84 GPa and 21.90±3.96 GPa for the Young's modulus, and 2.67±0.57% and 3.60±0.95 for the strain at failure, respectively. These values are very close to the ones obtained by Weibull distribution: ultimate tensile strength 142.8 MPa and 573.7 MPa, Young's modulus 6.43 GPa and 23.41 GPa, and strain at failure 2.87 % and 3.93%, respectively, with precision adjustment R-Squared values ranging from 0.953 to 0.981.

In addition, the tensile strength value obtained for VBs was similar to the one reported for agave fiber (135±71 MPa) (Bezazi et al., 2014), fiber fruit bunch branch of palm date (117±35 MPa) (Amroune et al., 2015) and *Juncus effusus L.* (113±36 MPa) (Maache et al., 2017). It is much higher for FSs (530.5±115.2 MPa), which value is close to the one reported for pineapple leaf fiber strands (506 MPa) (Mohamed et al., 2010), Prosopis juliflora bark fiber (558±13.4 MPa) (Saravanakumar et al., 2013) and sisal fiber (605.86 MPa) (Wei & Meyer, 2015). These results expressly demonstrated that the tensile properties are influenced mainly by the morphological structure and that the presence of the main voids decreases their properties. It can also be seen from the results that the tensile properties are increased with the increase in the crystallinity index of the fibers.

410

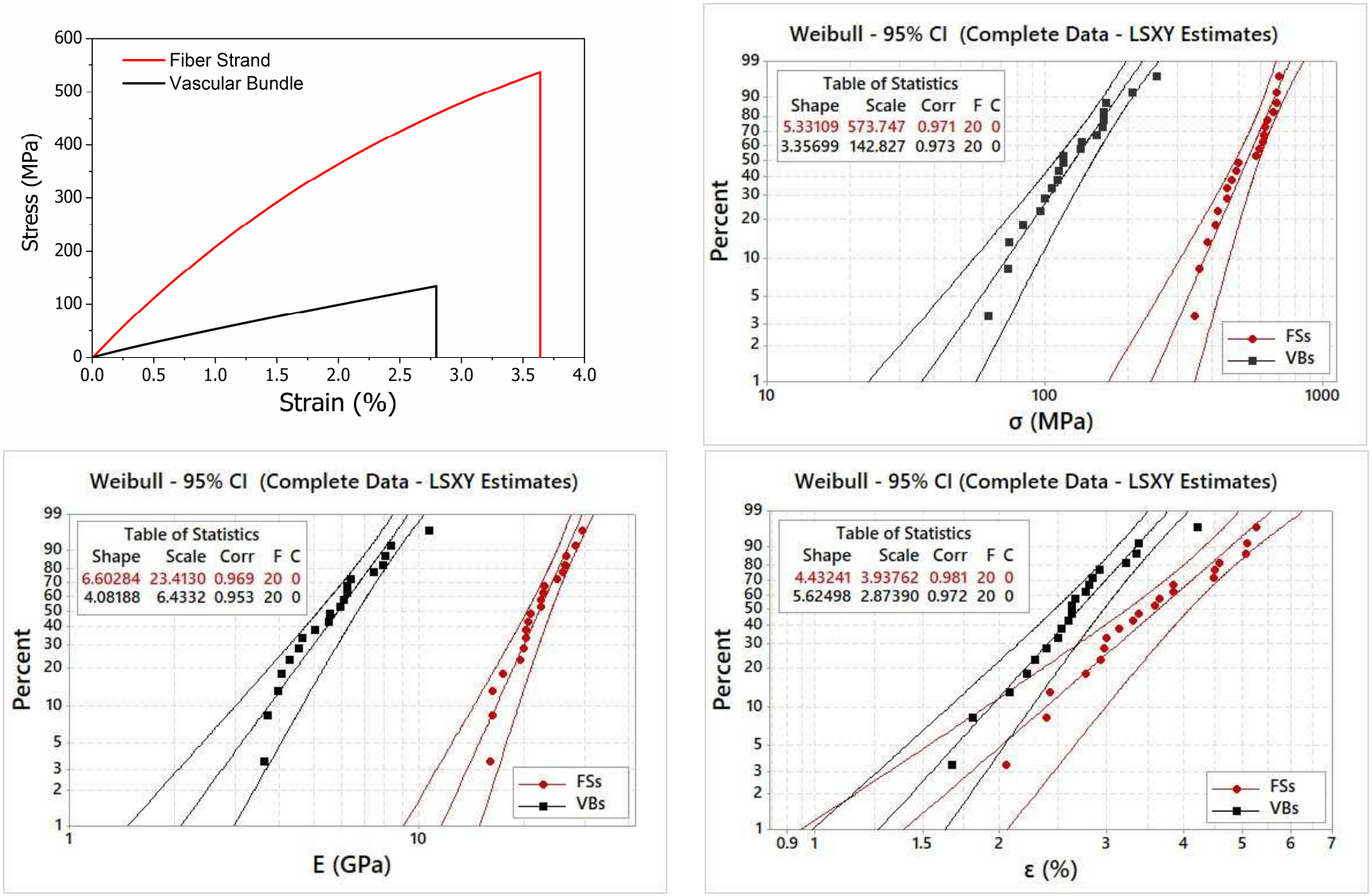

411

412 **Figure 8.** (a)Typical stress–strain curve for VBs and FSs, and two-parameter Weibull distribution for VBs and FSs for (b) tensile strength, (c)

413 Young's modulus, and (d) strain at break.

CONCLUSION

The investigation of the Ghars date palm rachis fibers leads to the main following conclusions:

- The existence of two main types of Ghars date palms rachis fibers have been identify, for the first time, on the basis of cross-sectional geometry namely: vascular bundles (VBs) and fiber strands (FSs) and showing their location in the rachis. Also, a new extraction method for Ghars rachis has been developed without any damaging or breaking it.
- The noncontact 3D profiler observations show that VBs and FSs have a rough surface (Ra=3.40 and Ra= 0.251, respectively), which is essential for adhesion to the polymer matrix.
- XRD analysis showed that FSs has a higher crystallinity index (56.68%) compared to VBs (47.82%). In addition, the crystallite size (CS) for VBs and FSs was found to be 5.78 nm and 5.63 nm, respectively.
- The main chemical and molecular structure groups were identified by FTIR analysis showing similar functional groups compared to other lignocellulosic fibers reported in the literature and EDX indicates similar composition content for both fibers.
- TGA and DSC analysis for VBs and FSs show that it can be stable up to 230 °C and 220, respectively, i.e. it has good thermal stability. The thermal events associated to hemicellulose, cellulose, and lignin has been determined.
- The density was evaluated for at 0.914 g/cm^3 for VBs, which was slightly lower that for FSs (0.922 g/cm^3).
- The statistical analysis with Weibull distribution function showed a good approximation fit value with the experimental data obtained. Thes results clearly indicate the effect of the crystallinity index and the structural morphology of the fibers on the tensile properties. In other words, the high crystallinity index leads to have better tensile properties.
- The tensile strength for FSs was found to be 530.5 ±115.2 MPa, i.e. more than 4 times than

for VBs (129.1 ±47.3 MPa),-and the Young's modulus of FSs and VBs was 21.90 ±3.96 GPa, 5.88 ±1.84 GPa, respectively.

- The mechanical properties obtained show high ultimate tensile stress for FSs compared to VBs and also to all the fibers date palm existing in the literature. Therefore, the fibers investigated show great potential for use as reinforcement for biocomposites in diverse engineering applications.

REFERENCES

Agoudjil, B., Benchabane, A., Boudenne, A., Ibos, L., & Fois, M. (2011). Renewable materials to reduce building heat loss: Characterization of date palm wood. *Energy and Buildings*, *43*(2–3), 491–497. https://doi.org/10.1016/j.enbuild.2010.10.014

Al-Kaabi, K., Al-Khanbashi, A., & Hammami, A. (2005). Date Palm Fibers as Polymeric Matrix Reinforcement : DPF / Polyester Composite Properties. *POLYMER COMPOSITES*, *26*, 604–613. https://doi.org/10.1002/pc.20130

Al-Khanbashi, A., Al-Kaabi, K., & Hammami, A. (2005). Date palm fibers as polymeric matrix reinforcement: Fiber characterization. *Polymer Composites*, *26*(4), 486–497. https://doi.org/10.1002/pc.20118

Al-oqla, F. M., Alothman, O. Y., Jawaid, M., Sapuan, S. M., & Es-Saheb, M. H. (2014). Processing and Properties of Date Palm Fibers and Its Composites. In *Biomass and Bioenergy* (pp. 1–25). Springer, Cham. https://doi.org/10.1007/978-3-319-07641-6

Al-Oqla, F. M., & Sapuan, S. M. (2014). Natural fiber reinforced polymer composites in industrial applications: Feasibility of date palm fibers for sustainable automotive industry. *Journal of Cleaner Production*, *66*, 347–354. https://doi.org/10.1016/j.jclepro.2013.10.050

Alawar, A., Hamed, A. M., & Al-Kaabi, K. (2009). Characterization of treated date palm tree fiber as composite reinforcement. *Composites Part B: Engineering*, *40*(7), 601–606. https://doi.org/10.1016/j.compositesb.2009.04.018

Almi, K., Lakel, S., Benchabane, a., & Kriker, a. (2015). Characterization of Date Palm Wood Used as Composites Reinforcement. *Acta Physica Polonica A*, *127*(4), 1072–1074. https://doi.org/10.12693/APhysPolA.127.1072

Alsaeed, T., Yousif, B. F., & Ku, H. (2013). The potential of using date palm fibres as

reinforcement for polymeric composites. *Materials and Design*, *43*, 177–184. https://doi.org/10.1016/j.matdes.2012.06.061

Amroune, S., Bezazi, A., Belaadi, A., Zhu, C., Scarpa, F., Rahatekar, S., & Imad, A. (2015). Tensile mechanical properties and surface chemical sensitivity of technical fibres from date palm fruit branches (Phoenix dactylifera L.). *Composites Part A: Applied Science and Manufacturing*, *71*(November), 98–106. https://doi.org/10.1016/j.compositesa.2014.12.011

Anwar, Z., Gulfraz, M., & Irshad, M. (2014). Agro-industrial lignocellulosic biomass a key to unlock the future bio-energy: A brief review. *Journal of Radiation Research and Applied Sciences*, *7*(2), 163–173. https://doi.org/10.1016/j.jrras.2014.02.003

Belaadi, A., Bezazi, A., Bourchak, M., Scarpa, F., & Zhu, C. (2014). Thermochemical and statistical mechanical properties of natural sisal fibres. *Composites Part B: Engineering*, *67*, 481–489. https://doi.org/10.1016/j.compositesb.2014.07.029

Bezazi, A., Belaadi, A., Bourchak, M., Scarpa, F., & Boba, K. (2014). Novel extraction techniques, chemical and mechanical characterisation of Agave americana L. natural fibres. *Composites Part B: Engineering*, *66*, 194–203. https://doi.org/10.1016/j.compositesb.2014.05.014

Biglari, F., AlKarkhi, A. F. M., & Easa, A. M. (2008). Antioxidant activity and phenolic content of various date palm (Phoenix dactylifera) fruits from Iran. *Food Chemistry*, *107*(4), 1636–1641. https://doi.org/10.1016/J.FOODCHEM.2007.10.033

Bouguedoura, N., Bennaceur, M., Babahani, S., & Benziouche, S. E. (2015). Date Palm Status and Perspective in Algeria. In *Date Palm Genetic Resources and Utilization: Volume 1: Africa and the Americas* (pp. 1–546). https://doi.org/10.1007/978-94-017-9694-1

Boumediri, H., Bezazi, A., Haddad, A., Saaidia, A., Scarpa, F., & Dufrsene, A. (2017). Physico-Chemical Characterization of Date Palm leaves (Phoenix Dactylifera-L) of Algeria. In A. J. M. Ferreira, E. Viola, F. Tornabene, & N. Fantuzzi (Eds.), *Mechcomp3: 3rd International Conference of Mechanics of Composite* (p. 24). Esculapio.

Chandrasekaran, M., & Bahkali, A. H. (2013). Valorization of date palm (Phoenix dactylifera) fruit processing by-products and wastes using bioprocess technology - Review. *Saudi Journal of Biological Sciences*, *20*(2), 105–120. https://doi.org/10.1016/j.sjbs.2012.12.004

Chao, C. C. T., & Krueger, R. R. (2007). The date palm (Phoenix dactylifera L.): Overview of biology, uses, and cultivation. *HortScience*, *42*(5), 1077–1082.

Darwish, E. A., Mansour, Y. M., & Elmously, H. (2018). Date Palm Rachis as a Local and Renewable Structural Material for Rural Communities in Egypt. *The International Journal of Environmental Science & Sustainable Development*, *2*(1), 1–11. https://doi.org/10.21625/essd.v2i1.173.g75

Fiore, V., Scalici, T., & Valenza, A. (2014). Characterization of a new natural fiber from Arundo donax L. as potential reinforcement of polymer composites. *Carbohydrate Polymers*, *106*(1), 77–83. https://doi.org/10.1016/j.carbpol.2014.02.016

Ghnimi, S., Umer, S., Karim, A., & Kamal-Eldin, A. (2017). Date fruit (Phoenix dactylifera L.): An underutilized food seeking industrial valorization. *NFS Journal*, *6*, 1–10. https://doi.org/10.1016/j.nfs.2016.12.001

Jawaid, M., & Abdul Khalil, H. P. S. (2011). Cellulosic/synthetic fibre reinforced polymer hybrid composites: A review. *Carbohydrate Polymers*, *86*(1), 1–18. https://doi.org/10.1016/j.carbpol.2011.04.043

Jayaramudu, J., Guduri, B. R., & Varada Rajulu, A. (2010). Characterization of new natural cellulosic fabric Grewia tilifolia. *Carbohydrate Polymers*, *79*(4), 847–851. https://doi.org/10.1016/j.carbpol.2009.10.046

Jebadurai, S. G., Raj, R. E., Sreenivasan, V. S., & Binoj, J. S. (2018). Comprehensive characterization of natural cellulosic fiber from Coccinia grandis stem. *Carbohydrate Polymers*, *207*, 675–683. https://doi.org/10.1016/j.carbpol.2018.12.027

Kambli, N., Basak, S., Samanta, K. K., & Deshmukh, R. R. (2016). Extraction of Natural Cellulosic Fibers from Cornhusk and Its Physico-Chemical Properties. *Fibers and Polymers*, *17*(5), 687–694. https://doi.org/10.1007/s12221-016-5416-0

Khiari, R., Mhenni, M. F., Belgacem, M. N., & Mauret, E. (2010). Chemical composition and pulping of date palm rachis and Posidonia oceanica - A comparison with other wood and non-wood fibre sources. *Bioresource Technology*, *101*(2), 775–780. https://doi.org/10.1016/j.biortech.2009.08.079

Maache, M., Bezazi, A., Amroune, S., Scarpa, F., & Dufresne, A. (2017). Characterization of a novel natural cellulosic fiber from Juncus effusus L. *Carbohydrate Polymers*, *171*, 163–172. https://doi.org/10.1016/j.carbpol.2017.04.096

Mallaki, M., & Fatehi, R. (2014). Design of a biomass power plant for burning date palm waste to cogenerate electricity and distilled water. *Renewable Energy*, *63*, 286–291. https://doi.org/10.1016/j.renene.2013.09.036

Manimaran, P., Saravanakumar, S. S., Mithun, N. K., & Senthamaraikannan, P. (2016). Physicochemical properties of new cellulosic fibers from the bark of Acacia arabica.

538 *International Journal of Polymer Analysis and Characterization*, *21*(6), 548–553.
539 https://doi.org/10.1080/1023666X.2016.1177699
540 Manimaran, P., Senthamaraikannan, P., Sanjay, M. R., Marichelvam, M. K., & Jawaid, M.
541 (2018). Study on characterization of Furcraea foetida new natural fiber as composite
542 reinforcement for lightweight applications. *Carbohydrate Polymers*, *181*, 650–658.
543 https://doi.org/10.1016/j.carbpol.2017.11.099
544 Martin, A. R., Martins, M. A., Da Silva, O. R. R. F., & Mattoso, L. H. C. (2010). Studies on
545 the thermal properties of sisal fiber and its constituents. *Thermochimica Acta*, *506*(1–2),
546 14–19. https://doi.org/10.1016/j.tca.2010.04.008
547 Mayandi, K., Rajini, N., Pitchipoo, P., Jappes, J. T. W., & Rajulu, A. V. (2016). Analysis and
548 Extraction and characterization of new natural lignocellulosic fiber Cyperus pangorei.
549 *International Journal of Polymer Analysis and Characterization*, *21*(2), 175–183.
550 https://doi.org/10.1080/1023666X.2016.1132064
551 Mayandi, K., Rajini, N., Pitchipoo, P., Sreenivasan, V. S., Jappes, J. W., & Alavudeen, A.
552 (2015). A comparative study on characterisations of Cissus quadrangularis and Phoenix
553 reclinata natural fibres. *Journal of Reinforced Plastics and Composites*, *34*(4), 269–280.
554 https://doi.org/10.1177/0731684415570045
555 Mohamed, A. R., Sapuan, S. M., Shahjahan, M., & Khalina, A. (2010). Effects of simple
556 abrasive combing and pretreatments on the properties of pineapple leaf fibers (palf) and
557 palf-vinyl ester composite adhesion. *Polymer - Plastics Technology and Engineering*,
558 *49*(10), 972–978. https://doi.org/10.1080/03602559.2010.482072
559 Nasser, R., Salem, M., Hiziroglu, S., Al-Mefarrej, H., Mohareb, A., Alam, M., & Aref, I.
560 (2016). Chemical Analysis of Different Parts of Date Palm (Phoenix dactylifera L.)
561 Using Ultimate, Proximate and Thermo-Gravimetric Techniques for Energy Production.
562 *Energies*, *9*(5), 374. https://doi.org/10.3390/en9050374
563 Oushabi, A., Sair, S., Oudrhiri Hassani, F., Abboud, Y., Tanane, O., & El Bouari, A. (2017).
564 The effect of alkali treatment on mechanical, morphological and thermal properties of
565 date palm fibers (DPFs): Study of the interface of DPF–Polyurethane composite. *South*
566 *African Journal of Chemical Engineering*, *23*, 116–123.
567 https://doi.org/10.1016/j.sajce.2017.04.005
568 Rabetafika, H. N., Bchir, B., Blecker, C., & Richel, A. (2014). Fractionation of apple by-
569 products as source of new ingredients: Current situation and perspectives. *Trends in*
570 *Food Science and Technology*, *40*(1), 99–114. https://doi.org/10.1016/j.tifs.2014.08.004
571 Roy, A., Chakraborty, S., Kundu, S. P., Basak, R. K., Basu Majumder, S., & Adhikari, B.

(2012). Improvement in mechanical properties of jute fibres through mild alkali treatment as demonstrated by utilisation of the Weibull distribution model. *Bioresource Technology*, *107*, 222–228. https://doi.org/10.1016/j.biortech.2011.11.073

Saadaoui, N., Rouilly, A., Fares, K., & Rigal, L. (2013). Characterization of date palm lignocellulosic by-products and self-bonded composite materials obtained thereof. *Materials and Design*, *50*, 302–308. https://doi.org/10.1016/j.matdes.2013.03.011

Saravanakumar, S. S., Kumaravel, A., Nagarajan, T., & Moorthy, I. G. (2014). Effect of Chemical Treatments on Physicochemical Properties of Prosopis juliflora Fibers. *International Journal of Polymer Analysis and Characterization*, *19*(5), 383–390. https://doi.org/10.1080/1023666X.2014.903585

Saravanakumar, S. S., Kumaravel, A., Nagarajan, T., Sudhakar, P., & Baskaran, R. (2013). Characterization of a novel natural cellulosic fiber from Prosopis juliflora bark. *Carbohydrate Polymers*, *92*(2), 1928–1933. https://doi.org/10.1016/j.carbpol.2012.11.064

Segal, L., Creely, J. J., Martin, A. E., & Conrad, C. M. (1959). An Empirical Method for Estimating the Degree of Crystallinity of Native Cellulose Using the X-Ray Diffractometer. *Textile Research Journal*, *29*(10), 786–794. https://doi.org/10.1177/004051755902901003

Wei, J., & Meyer, C. (2015). Degradation mechanisms of natural fiber in the matrix of cement composites. *Cement and Concrete Research*, *73*, 1–16. https://doi.org/10.1016/j.cemconres.2015.02.019